J Mater Sci: Mater Med (2012) 23:2981–2992
DOI 10.1007/s10856-012-4758-4

Bone-bonding properties of Ti metal subjected to acid and heat treatments

Toshiyuki Kawai · Mitsuru Takemoto · Shunsuke Fujibayashi · Masashi Neo · Haruhiko Akiyama · Seiji Yamaguchi · Deepak K. Pattanayak · Tomiharu Matsushita · Takashi Nakamura · Tadashi Kokubo

Received: 25 July 2012 / Accepted: 23 August 2012 / Published online: 5 September 2012

Abstract The effects of surface treatment on the bone-bonding properties of Ti metal were examined by both mechanical detaching test and histological observation after implantation into rabbit tibiae for various periods ranging from 4 to 26 weeks. The bone-bonding ability of Ti metal, which is extremely low as it is abraded, was hardly increased by simple heat treatment at 600 °C or treatment with H_2SO_4/HCl mixed acid alone, but was markedly increased by the heat treatment after the acid treatment. Even Ti metal that had been previously subjected to NaOH treatment showed considerably high bone-bonding ability after acid and heat treatments. Such high bonding abilities were attributed to their high apatite-forming ability in the body environment. Their high apatite-forming abilities were attributed to a high positive surface charge, and not to the type of crystalline phase or specific roughness of their surfaces. The present study has demonstrated that acid and subsequent heat treatments are effective for conferring stable fixation properties on Ti metal implants.

T. Kawai (✉) · M. Takemoto · S. Fujibayashi · M. Neo · H. Akiyama
Department of Orthopaedic Surgery, Graduate School of Medicine, Kyoto University, 54 Kawahara-cho, Shougoin, Sakyou-ku, Kyoto, Japan
e-mail: kawait@kuhp.kyoto-u.ac.jp

S. Yamaguchi · D. K. Pattanayak · T. Matsushita · T. Kokubo
Department of Biomedical Science, College of Life and Health Science, Chubu University, 1200 Matsumoto-cho, Kasugai, Aichi, Japan

T. Nakamura
National Hospital Organization Kyoto Medical Center, 1-1 Mukaihata-cho, Fukakusa, Fushimi-ku, Kyoto, Japan

1 Introduction

Metallic materials, such as Ti metal and its alloys, are widely used for various implants in the orthopedic and dental fields because of their high fracture toughness and good biocompatibility. However, they do not bond to living bone. When implanted into a bone defect, polished or abraded Ti metal subjected to no additional treatment becomes encapsulated by fibrous tissue, and thus becomes isolated from the surrounding bone, [1, 2]. To address this problem, the metal is often coated with bioactive ceramics to provide bone-bonding ability. One of the most accepted and commercialized bioactive coating materials is plasma-sprayed hydroxyapatite (HA) [3–6]. However, although many good clinical results have been reported, a number of problems related to its low fatigue strength, degradation and delamination during long-term implantation have become apparent. HA particles, when generated near an artificial joint surface, cause third-body wear leading to excessive polyethylene wear and osteolysis [7, 8]. For these reasons, HA-coated implants need to be continuously monitored by radiography.

On the other hand, it has been reported that Ti metal bonds to living bone if subjected to NaOH and heat treatments to form sodium titanate on its surface, since it forms an apatite layer on its surface in the living body [9–12]. These treatments have been applied to the porous Ti metal layer on a total hip joint, and this joint has been used clinically in Japan since 2007 [13].

Apatite formation on NaOH- and heat-treated Ti metal in vivo has been reproduced even in simulated body fluid (SBF) with ion concentrations almost equal to those in human blood plasma [14, 15]. Recently, it was shown that Ti metal subjected to H_2SO_4/HCl mixed acid and subsequent heat treatments also formed apatite on its surface in

SBF [16], and that even Ti metal previously subjected to NaOH treatment formed apatite on its surface in SBF after subsequent acid and heat treatments, irrespective of the type of acid solution employed [17]. These findings indicate that Ti metal subjected to acid and heat treatments can also bond tightly to living bone. With regard to the response of tissues to these Ti metals, only preliminary results of animal experiments using Ti metal subjected to the mixed-acid and heat treatments have been briefly reported [16].

In the present study, we examined the bone-bonding properties of Ti metal subjected to different acid and heat treatments using mechanical detaching test and histological observation after implantation into rabbit tibiae for various period of time ranging from 4 to 26 weeks, in comparison with those of Ti metals that had been simply abraded, heat-treated or acid-treated. The bone-bonding properties were discussed in terms of apatite-forming ability in SBF, which in turn were discussed in terms of their surface structures and properties.

It is believed that studies of this type are useful for expanding the range of available bone-bonding metals, and also for gaining a fundamental understanding of the factors governing the bone-bonding properties of Ti metal.

2 Materials and methods

2.1 Preparation of Ti metal samples

Six kinds of Ti metal samples were used: abraded titanium plates (Ab), plates that had been abraded and heat-treated (AbH), plates that had been treated with mixed acid (MA), plates that had been treated with the same mixed acid and then heat-treated (MAH), plates that had been initially treated with NaOH, then immersed in 0.5 mM HCl, and finally heat-treated (0.5HCl-H), and plates that had been initially treated with NaOH, then immersed in 50 mM HCl, and finally heat-treated (50HCl-H).

The technical details have been described previously [16, 18]. Commercial pure Ti metal (Kobe Steel, Japan, grade 2, O_2 content 0.15 wt %) was cut into rectangular samples (various sizes as needed for each of the experimental conditions), and abraded with a no. 400 diamond abrasive plate. All the abraded samples were washed with acetone, 2-propanol and ultrapure water for 30 min each in an ultrasonic cleaner, and then dried overnight in an oven at 40 °C. The plates in group Ab were produced by abrasion alone. In group AbH, the abraded plates were heated to a temperature of 600 °C at a rate of 5 °C min^{-1} in an Fe–Cr furnace in air (heat treatment). The plates were kept at this temperature for 1 h, and then allowed to cool to room temperature at the natural rate of the furnace. In group MA, abraded plates were soaked in 20 ml of a mixture of 66.3 % H_2SO_4 (w/w) solution (Kanto Chemical Co., Inc., Japan) and 10.6 % HCl (w/w) solution (Kanto Chemical Co., Inc.) in a weight ratio of 1:1 at 70 °C for 1 h in an oil bath shaken at 120 strokes min^{-1}, then gently washed with ultrapure water and dried overnight in an oven at 40 °C. In group MAH, the abraded plates were acid-treated using the same method as that for group MA, and then heated at 600 °C in the same way as that for group AbH.

For group 0.5HCl-H, the abraded titanium plates (the same as those used for group Ab) were immersed in 5 ml of aqueous 5 M NaOH solution at 60 °C for 24 h (alkali treatment), then in 0.5 mM HCl (pH 3.5) at 40 °C for 24 h, dried at room temperature for 24 h, and then heat-treated at 600 °C. For group 50HCl-H, 50 mM HCl (pH 1.5) was used instead of 0.5 mM HCl.

2.2 Surface analysis of Ti metal samples

The morphologies of the surfaces and cross-sections of the Ti metal samples subjected to various treatments were observed using a field-emission scanning electron microscope (SEM) (S-4700, Hitachi Ltd., Japan) at an acceleration voltage of 15 kV. The crystalline phases of the surfaces of the Ti metal samples subjected to various treatments were analyzed by thin-film X-ray diffraction (TF-XRD; RINT-2500, Rigaku Co., Japan).

2.3 Zeta potential measurements of Ti metal samples

Titanium metal plates (size: 13 × 33 × 1 mm^3) were prepared using the same method as that described in Sect. 2.1. One side of each treated Ti metal sample was earthed to allow for leakage of any stray charge, and then the sample was immediately set in a zeta potential and particle size analyzer (model ELS-Z1, Otsuka Electronics Co., Japan) using a glass cell. The zeta potential of the sample was measured under an applied voltage of 40 V in 10 mM NaCl solution. The dispersant monitoring particles of polystyrene latex (size: 500 nm) were coated with hydroxypropyl cellulose. Five samples were measured for each experimental condition, and the average value (±standard deviation: SD) was used.

2.4 Examination of the apatite-forming ability of Ti metal samples in SBF

The samples (size: 10 × 10 × 1 mm^3) were soaked in 30 ml of acellular SBF with ion concentrations nearly equal to those of human blood plasma at 36.5 °C (Na^+ = 142.0, K^+ = 5.0, Mg^{2+} = 1.5, Ca^{2+} = 2.5, Cl^- = 147.8, HCO_3^- = 4.2, HPO_4^{2-} = 1.0 and SO_4^{2-} = 0.5 mM [14, 15]). The SBF was

prepared by dissolving reagent grade NaCl, $NaHCO_3$, KCl, $K_2HPO_43H_2O$, $MgCl_26H_2O$, $CaCl_2$ and Na_2SO_4 (Nacalai Tesque Inc.). The samples were removed from the SBF after 1 day, gently washed with ultrapure water, dried in an oven at 40 °C, and coated with a Pt/Pd film. The formation of apatite on the sample surface was examined using SEM.

2.5 Examination of the bone-bonding ability of Ti metal samples

2.5.1 Implantation

The implants (size: 15 × 10 × 2 mm^3) were conventionally sterilized with ethylene oxide gas and implanted into the tibial metaphyses of mature male Japanese white rabbits weighing 2.8–3.2 kg. The surgical methods used have been described previously [19–23]. The rabbits were anesthetized with an intravenous injection of pentobarbital sodium (0.5 ml/kg) and local administration of a solution of 0.5 % lidocaine. After shaving, disinfection, and draping, a straight 3-cm skin incision was made over the medial side of the knee, and the fascia and periosteum were incised and retracted to expose the tibial cortex. Using a dental bur, a 16 × 2-mm^2 hole was created from the medial to the lateral cortex parallel to the longitudinal axis of the tibial metaphysis. After irrigation of the hole with saline, the titanium plates were implanted in a frontal direction, perforating the tibia and protruding from the medial to the lateral cortex (Fig. 1a). The fascia and skin were finally closed in layers. The surgical procedures were performed bilaterally. One randomly chosen plate was implanted into each tibia. At 4, 8, 16 and 26 weeks after implantation, the rabbits were euthanatized with an overdose of intravenous pentobarbital sodium. Eight implants were used per experimental condition. Among them, six were used for the detaching test, and the remaining two were used for histological analysis without the detaching test. This study was approved by the Animal Research Committee of the Graduate School of Medicine, Kyoto University, Japan.

2.5.2 Measurement of detaching failure load

Following euthanasia, segments of the proximal tibial metaphyses containing the implanted plates were retrieved and prepared for the detaching test. The bone tissue surrounding the plates was removed with a dental bur so that no anterior bone segment was connected directly to a posterior bone segment (Fig. 1b). Using an Instron-type autograph (Model 1011, Aikoh Engineering, Nagoya, Japan), traction was applied through hooks holding each bone segment at a cross-head speed of 35 mm/min (Fig. 1c). Care was taken so that strain was applied perpendicular to the surface of the implant. When the plate became detached from the bone, the load was recorded as the failure load. If the plate was already detached before the test, the failure load was recorded as 0 N. Six samples were analyzed for each type of implant after each implantation period. All data are expressed as mean ± standard deviation (SD) and were analyzed statistically according to the implant type using one-way ANOVA followed by post-hoc test (Tukey–Kramer multiple comparison test). Differences at $P < 0.05$ were considered statistically significant.

2.5.3 Histological examination

Two specimens from each group harvested after each time interval were allocated to histological analysis. The segments of the tibiae containing the implanted samples were fixed in 10 % phosphate-buffered formalin for 7 days, and dehydrated in serial concentrations of ethanol (70, 80, 90, 99, 100, and 100 % v/v) for 3 days at each concentration. Some sections with a thickness of 500 μm were cut, bound to a transparent acrylic plate, and ground to a thickness of 40–50 μm. These samples were stained using Stevenel's blue and Van Gieson's picro-fuchsin. Histological evaluation was performed on each stained section using a transmission light microscope (Eclipse 80i, Nikon Co., Japan).

2.5.4 Observation of surfaces after the detaching test

The samples after the detaching test were prepared for analysis of the implant surface. Specimens were washed in sodium hypochlorite solution to remove the soft tissue, fixed in 10 % phosphate-buffered formalin for 3 days, and dehydrated in serial concentrations of ethanol (70, 80, 90, 99, 100, and 100 % v/v) for 1 day at each concentration. The specimens were then soaked in isopentyl acetate solution for 1 day and dried in a critical-point drying apparatus (HCP-2, Hitachi, Tokyo, Japan). They were then coated with carbon and examined using a SEM with an attached energy-dispersive X-ray microanalyzer (SEM-EDX; EMAX-3000, Horiba, Kyoto, Japan).

2.5.5 Observation of surface structure immediately after implantation

Sample groups for examination of surface structure immediately after implantation were chosen on the basis of changes in surface structure after the detaching test. Ti metal plates were inserted into rabbit tibiae as described in Sect. 2.5.1, and then immediately retrieved by cutting the surrounding bone so that no further pressure or friction was applied to the plate surface. The retrieved samples were

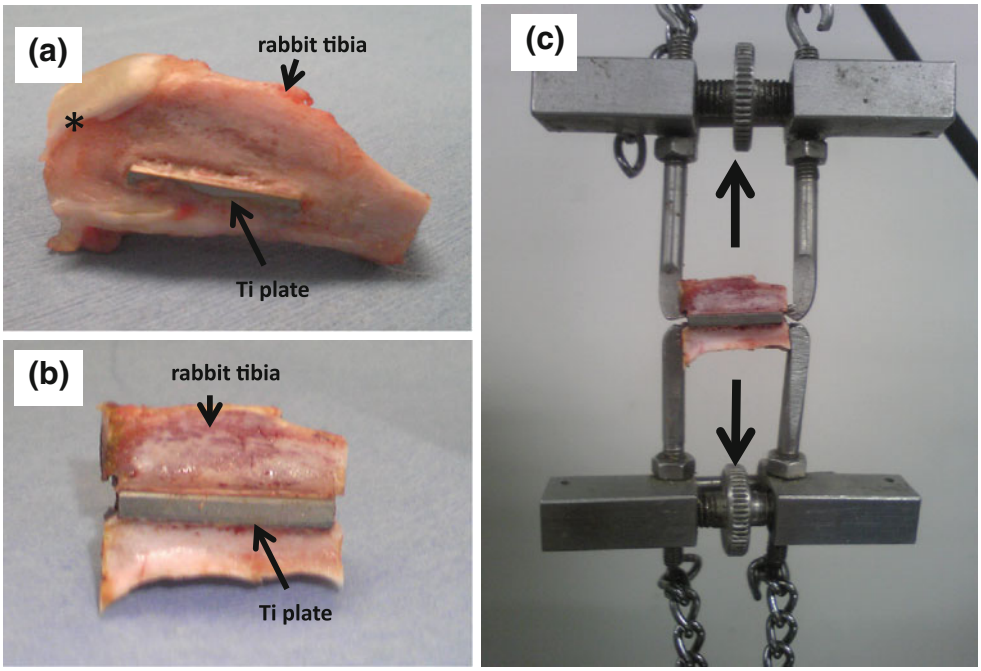

Fig. 1 Schematic drawings of the detaching test and preparation for the test. **a** Insertion of the titanium plate into the rabbit tibia. **b** The bone-plate-bone construct after cutting the tibia at the proximal and distal ends of the plate. **c** Tensile load was applied while holding the anterior and posterior cortices until detachment occurred

prepared in the same way as described in Sect. 2.5.4, and the surface was observed using SEM.

3 Results

3.1 Changes in the surface structure of Ti metal samples after various treatments

Figure 2 shows SEM photographs of the surfaces and cross-sections of the Ti metal plates before and after the chemical and heat treatments. The plates subjected to abrasion alone (group Ab) showed only scratches on the surface, and these scratches became a little dull after heat treatment (AbH). Only the Ti metal phase was detected on Ab by TF-XRD, while rutile of titanium oxide was detected besides the Ti metal phase on AbH.

The acid treatment produced micrometer-scale surface roughness on the plates (MA: shown in Fig. 2), and subsequent heat treatment did not change the surface structure appreciably (MAH in Fig. 2). TF-XRD detected titanium hydride besides the Ti metal on MA, while rutile as well as Ti metal was detected on MAH.

The plates subjected to HCl and heat treatments after the alkali treatment showed nanometer-scale surface roughness which is produced by fine feather-like phases about 1 micrometer thick. HCl concentrations of both 0.5 mM (0.5HCl-H) and 50 mM (50HCl-H) resulted in almost the same surface structure. The crystalline phases detected on 0.5HCl-H and 50HCl-H by TF-XRD were rutile (R) and anatase (A) of titanium oxide besides Ti metal, where the R/A ratio for 0.5HCl-H was much lower than that for 50HCl-H.

3.2 Zeta potential

Table 1 shows the zeta potential of each sample as mean ± SD. For the Ab and MA groups, which were not subjected to heat treatment, the zeta potentials were unmeasurable. This was presumably due to an excessively thin layer of insulating titanium oxide on their surface [16]. The AbH samples, which were heat-treated without being subjected to acid treatment, showed low zeta potentials of around zero, whereas the MAH, 0.5HCl-H and 50HCl-H samples, which had been heat-treated after acid treatment, showed positive zeta potentials.

3.3 Apatite formation

Figure 3 shows SEM photographs of the surfaces of Ti metal samples that had been soaked in SBF for 1 day. No deposit was observed on plates in the Ab, AbH or MA groups, whereas apatite formation was confirmed on plates in the MAH, 0.5HCl-H and 50HCl-H groups, which had been subjected to acid and subsequent heat treatments. The degree of apatite formation on 50HCl-H was greater than that on 0.5HCl-H.

3.4 Detaching test (failure load)

All of the rabbits tolerated the procedure well. No infection of the surgical site or dislocation of the implants was

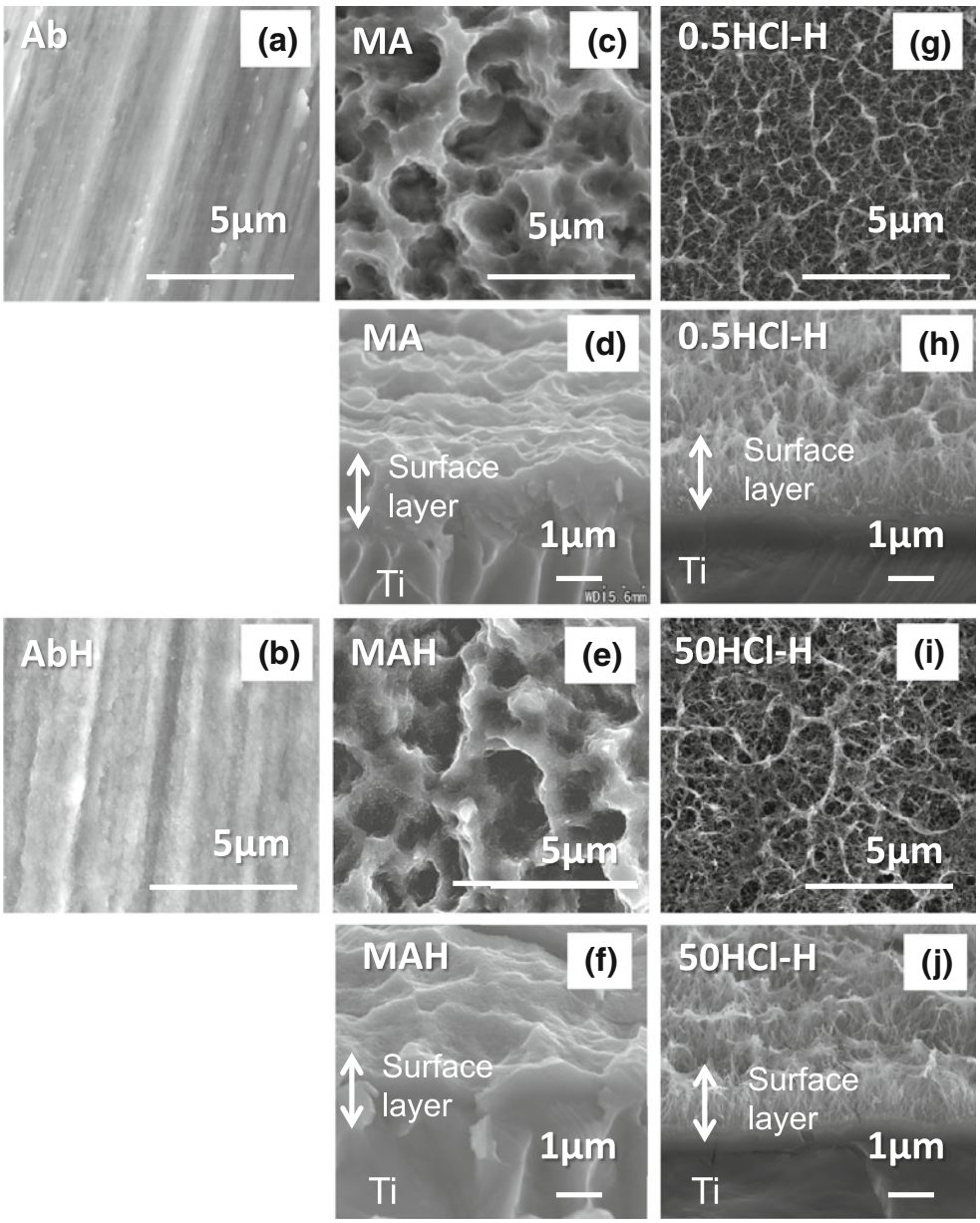

Fig. 2 SEM photographs of the surfaces and cross sections of Ti metal plates subjected to various treatments: **a** surface as-abraded, **b** surface only heat-treated, **c** surface only mixed-acid treated, **d** cross section only mixed-acid treated, **e** surface heat-treated after mixed-acid treatment, **f** cross section heat-treated after mixed-acid treatment, **g** surface 0.5 mM HCl and heat-treated after alkali treatment, **h** cross section. 0.5 mM HCl and heat-treated after alkali treatment, **i** surface 50 mM HCl and heat-treated after alkali treatment and **j** cross section. 50 mM HCl and heat-treated after alkali treatment

Table 1 zeta potential measurement

Type of plate	Treatment	Zeta potential
Ab	Abraded only	Unmeasurable (considered zero)
AbH	Heat treatment alone	−2.1 (±3.1)mV
MA	Mixed acid treatment alone	Unmeasurable (considered zero)
MAH	Mixed acid and heat treatment	+4.8 (±1.3)mV
0.5HCl-H	NaOH, 0.5 mM HCl and heat treatment	+3.4 (±2.3)mV
50HCl-H	NaOH, 50 mM HCl and heat treatment	+8.4 (±1.8)mV

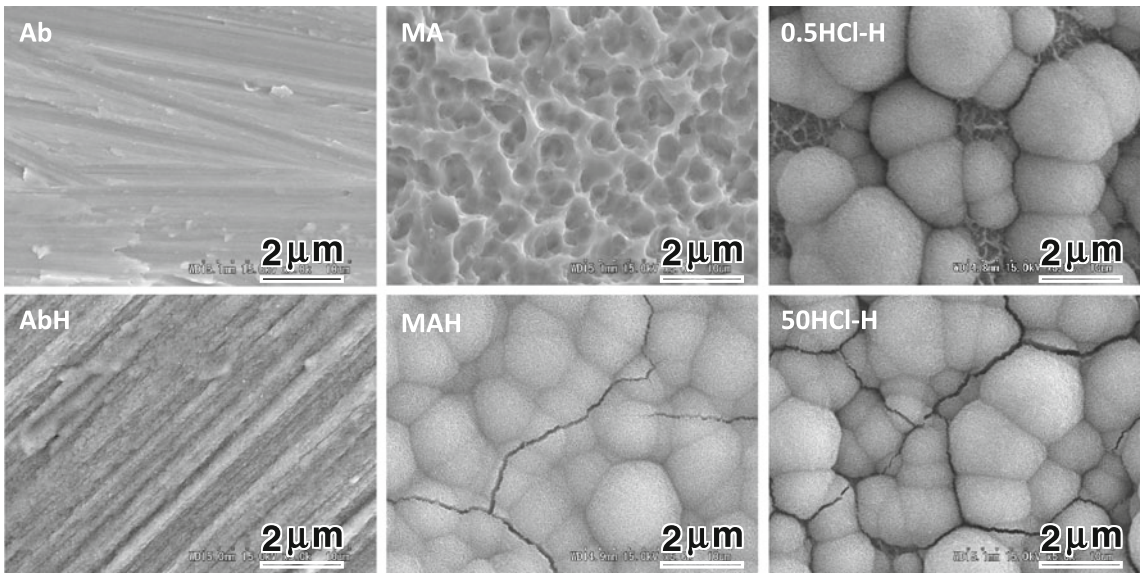

Fig. 3 SEM photographs of the surfaces of Ti metal subjected to various treatments and soaked in SBF for one day

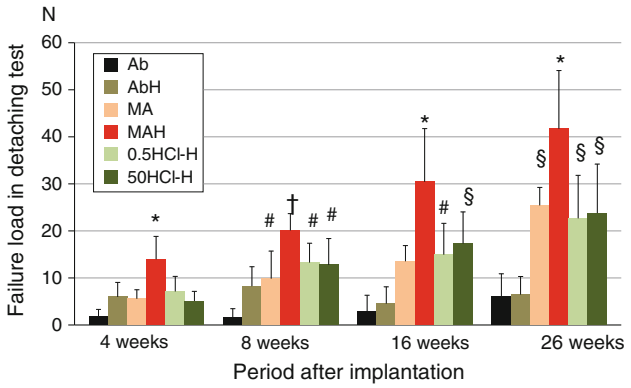

Fig. 4 Failure load in the detaching test for Ti metal subjected to various treatments after implantation for different periods. (Error bar: standard deviation) (N). *$P < 0.05$ vs Ab, AbH, MA, 0.5HCl-H, and 50HCl-H, †$P < 0.05$ vs Ab, AbH, and MA, §$P < 0.05$ vs Ab and AbH, #$P < 0.05$ vs Ab

observed upon dissection after euthanasia. No apparent adverse reactions such as inflammation or foreign-body reactions were noted on or around any of the implanted plates. The changes in detaching failure loads for each material at 4, 8, 16, and 26 weeks after implantation are summarized in Fig. 4. Hereafter, the failure loads are given as mean (±standard deviation). At 4 weeks, the failure loads were 1.73 (±1.57) N for Ab, 5.95 (±3.10) N for AbH, 5.57 (±1.91) N for MA, 14.0 (±4.84) N for MAH, 7.13 (±3.20) N for 0.5HCl-H, and 5.10 (±2.05) N for 50HCl-H samples ($n = 6$). At 8 weeks, they were 2.05 (±1.91) N, 7.18 (±4.53) N, 9.85 (±5.87) N, 20.1 (±3.55) N, 13.2 (±4.12) N, and 12.8 (±5.60) N, respectively ($n = 6$), and at 16 weeks, 3.18 (±3.14) N, 4.20 (±3.29) N, 13.6 (±3.32) N, 30.4 (±11.3) N, 15.0 (±6.67) N, 17.3 (±6.70) N, respectively ($n = 6$). At 26 weeks, the corresponding values were 5.97 (±4.36) N, 6.42 (±3.44) N, 25.4 (±3.81) N, 41.7 (±12.4) N, 22.7 (±9.13) N, and 23.8 (±10.4) N, respectively.

At 4 weeks, the failure load for MAH was significantly higher than that for Ab ($P < 0.0001$), AbH ($P = 0.002$), MA ($P = 0.001$), 0.5HCl-H ($P = 0.01$) or 50HCl-H ($P = 0.0005$). Except for MAH, no combinations of two groups showed any significant difference in failure load at 4 weeks.

The failure load in the MAH group was significantly higher than that in any other group at 4, 16 and 26 weeks ($P < 0.05$). The failure load in the MAH group was also significantly higher than that in the MA group at every time point.

In contrast, the failure load in the Ab group was the lowest among the six groups; however, there was no significant difference between the failure load in group Ab and that in group AbH at any of the time points.

There was no significant difference between the failure loads in the 0.5HCl-H and 50HCl-H groups at any time point. Both the 0.5HCl-H and 50HCl-H groups showed a significantly lower failure load than the MAH group at 4, 8, and 26 weeks.

3.5 Histological examination

Representative histological images of each sample group are shown in Fig. 5 (at 4 weeks) and Fig. 6 (at 8 weeks). In the samples from the MAH, 0.5HCl-H and 50HCl-H groups, new bone had formed in the gap at the implantation site within 4 weeks, and a large amount of new bone was in contact with the surface (Fig. 5). In the samples from the

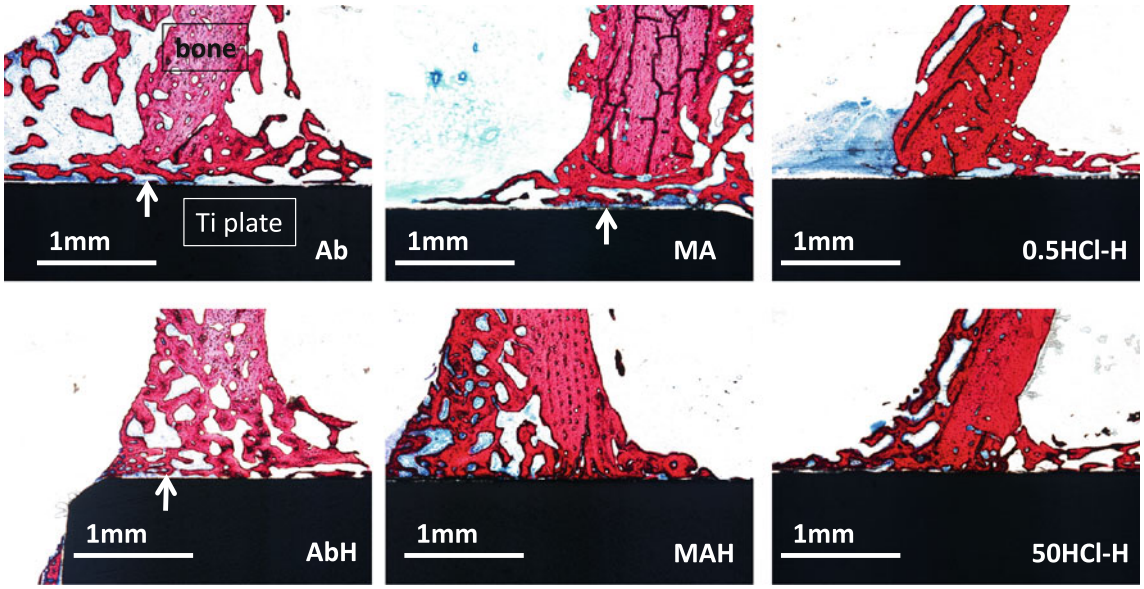

Fig. 5 Non-decalcified histological sections of each implant after implantation for 4 weeks. Stain: Stevenel's blue and Van Gieson's picrofuchsin. *White arrows* indicate a gap between the Ti metal and new bone

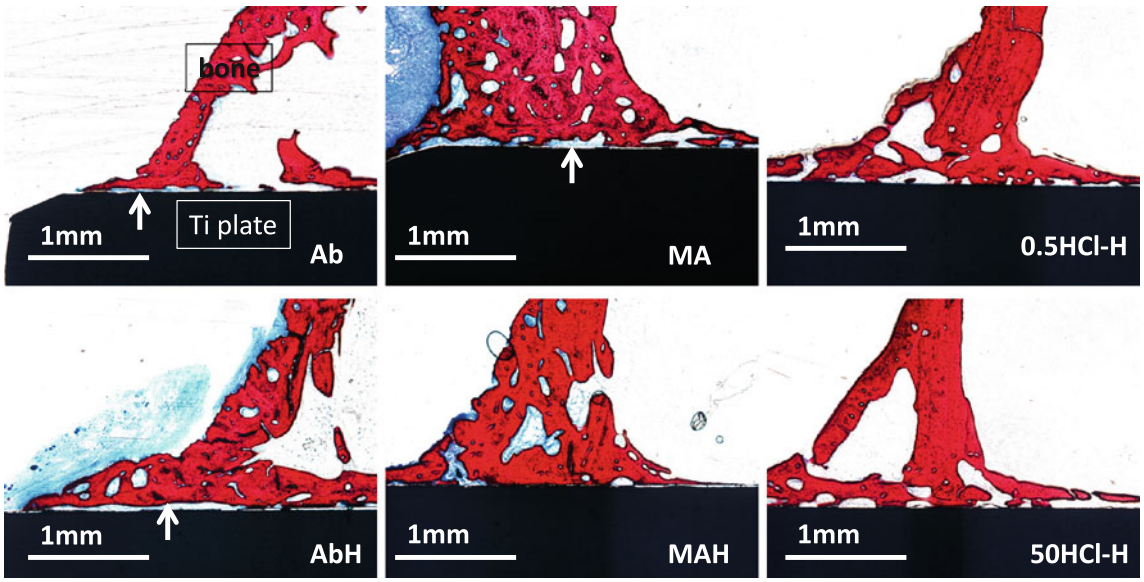

Fig. 6 Non-decalcified histological sections of each implant after implantation for 8 weeks. Stain: Stevenel's blue and Van Gieson's picrofuchsin. *White arrows* indicate a gap between the Ti metal and new bone

MA group, a relatively small amount of bone was in direct contact at 4 weeks, as compared with the MAH group. The amount of new bone formation in the gap in the 0.5HCl-H group appeared similar to that in the 50HCl-H group, and the amount of bone in direct contact in the 0.5HCl-H and 50HCl-H groups was relatively small in comparison with the MAH group. The samples in the Ab, AbH and MA groups had an intervening layer of soft tissue between the bone and the implant throughout the examined period. These histological findings were consistent with the results of mechanical testing.

Newly formed bone in the Ab, AbH, and MA groups also seemed to be characterized by haphazard organization of collagen fibers, whereas that in the MAH, 0.5HCl-H and 50HCl-H groups showed a more regular parallel alignment of collagen fibers. This implies that the surface environment of the samples in the MAH, 0.5HCl-H and 50HCl-H groups had more mature bone than the other samples. At 8 weeks,

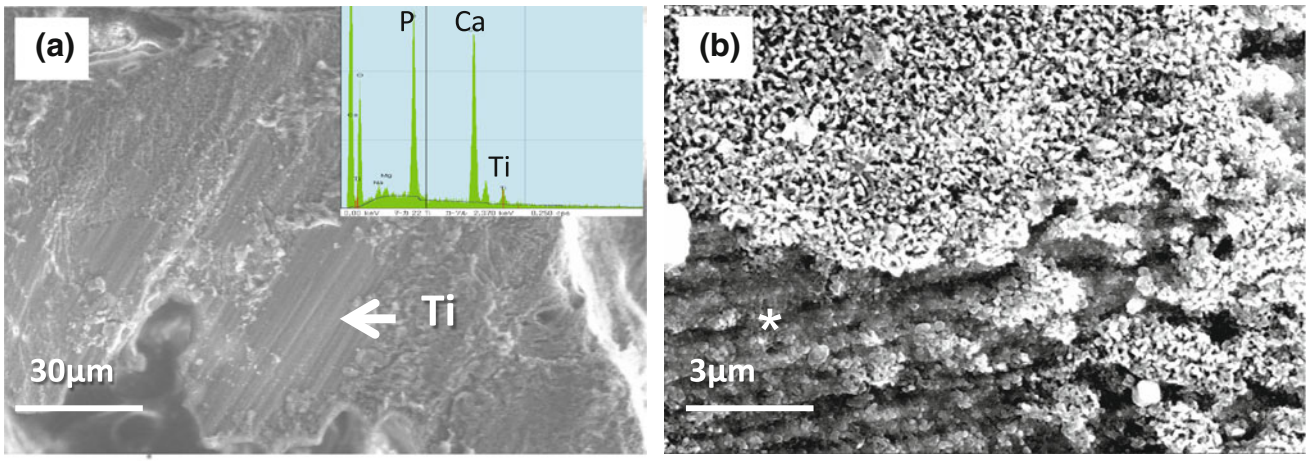

Fig. 7 SEM examination of the surface of a 0.5HCl-H sample after the detaching test at 4 weeks. **a** On the detached bone, detached titanium layers are evident (*white arrow*). The graph at the top right shows the result of EDX examination indicating Ti metal on the surface. **b** The surface network was partly detached and the Ti metal substrate was exposed (*asterisk*)

the newly formed bone had become remodeled and exhibited more organized collagen patterns in all samples; however, direct bonding between bone and the Ti plate was sparse in the Ab, AbH and MA groups (Fig. 6). Although at 8 weeks the samples in the 0.5HCl-H and 50HCl-H groups showed bone-bonding, that in the MAH group was more robust. At 16 and 26 weeks, the new bone had become more organized and remodeled in all of the groups.

3.6 Examination of the surface after the detaching test

At 4 weeks after implantation, a considerable amount of mature bone that was well integrated with the rough surface of the Ti plate remained in the MA, MAH, 0.5HCl-H and 50HCl-H groups after the detaching test (not shown in figures), indicating that breakage had occurred in the bone once bone contact had been established. In comparison with the MA, 0.5HCl-H and 50HCl-H groups, the MAH group showed a larger amount of bone on the surface. On the other hand, in the Ab and AbH groups, only a small amount of residual bone was evident on the surface of the implant after the detaching test.

On the surface of the plates subjected to 0.5HCl-H and 50HCl-H treatment, breakage of the surface layer and subsequent exposure of the substrate were observed after the detaching test at 4, 8, 16 and 26 weeks after implantation. After the detaching test, a mixture of bone residue, a surface layer with a nanometer-scale network structure, and the bare titanium substrate were partly evident on the surface of 0.5HCl-H plates (Fig. 7). The appearance of the plates at 4, 8, 16 and 26 weeks did not differ markedly. In the MA and MAH groups, no breakage was observed in the surface layer, and the rough structure of the surface layer remained unchanged at all time points after implantation. Similarly, the plates in the Ab and AbH groups showed no breakage in the surface layer at any time point after implantation. Consistent with this finding, observation of the bony surface after the detaching test demonstrated no Ti metal layer in the Ab, AbH, MA and MAH groups, indicating that the rough surface structure formed in the MA and MAH groups by mixed acid treatment was strong enough to withstand the detaching loads.

Observations of other parts of specimens in the 0.5HCl-H and 50HCl-H groups revealed a different form of change in the surface structure. Figure 8 shows that after the detaching test the fine network present before implantation was extensively lost in the 0.5HCl-H group, and a similar change was also evident on Ti plates in the 50HCl-H group.

3.7 Surface structure immediately after implantation

The surface structures of two groups (0.5HCl-H and 50HCl-H) were examined immediately after implantation using SEM. The surface structure of a MAH plate immediately after implantation was also observed as a control.

The surface structure of plates in the 0.5HCl-H group immediately after implantation (Fig. 9) appeared collapsed and leveled, being very similar to that observed after the detaching test at 4 weeks (Fig 8b), and to the surface structure seen in the 50HCl-H group immediately after implantation (not shown in figures). The surface structure of plates in the MAH group remained unchanged after implantation.

4 Discussion

It was apparent from the results of the detaching test and the histological observations described above that Ti metal that had been subjected to abrasion alone showed extremely low bone-bonding ability even at 26 weeks after implantation.

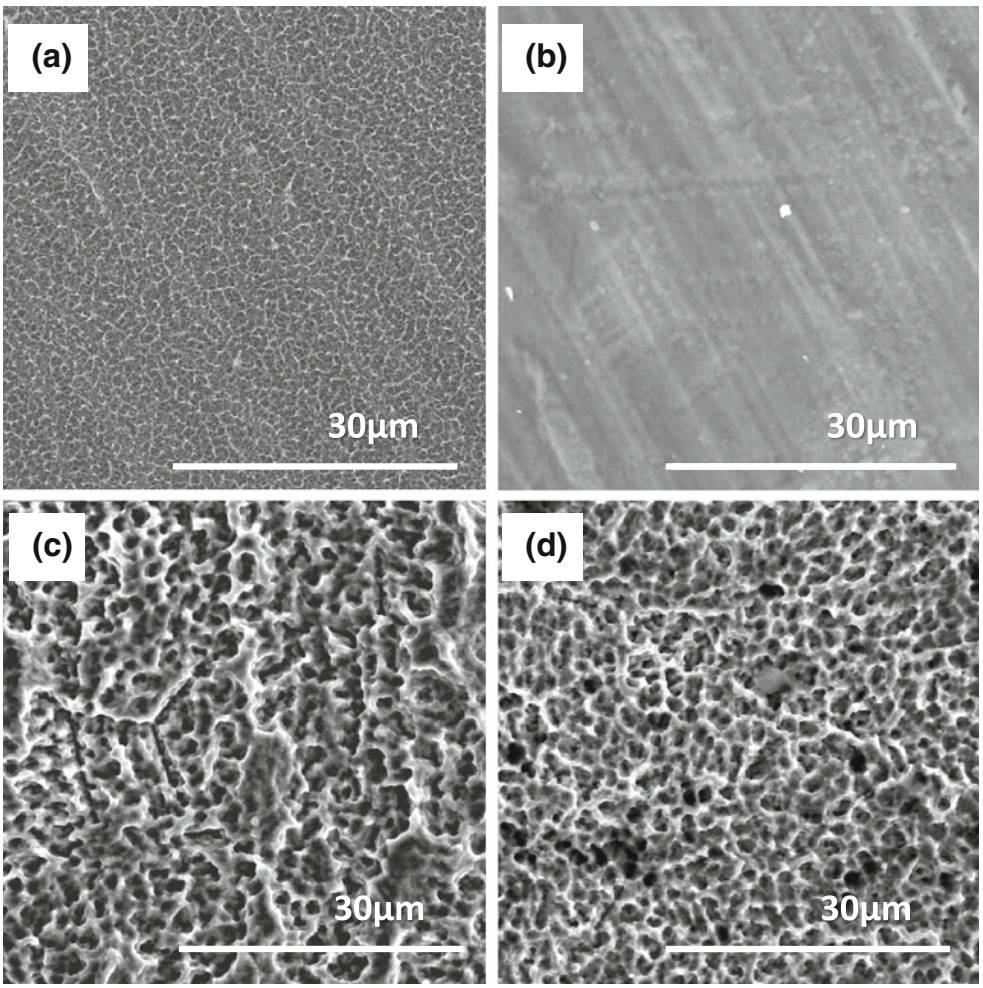

Fig. 8 SEM photographs of the surfaces of 0.5HCl-H and MAH samples. **a** 0.5HCl-H plate before implantation: a nanometer-scale network is evident. **b** 0.5HCl-H plate after the detaching test after implantation for 4 weeks: a leveled surface with loss of the nanometer-scale network is evident. **c** MAH plate before implantation: a micrometer-scale rough structure is evident. (d) MAH plate after the detach test at 4 weeks after implantation: the micrometer-scale surface structure remains unchanged

Simple heat treatment did not confer any appreciable increase in bone-bonding ability even at 26 weeks after implantation. Also, acid treatment resulted in no significant increase of bone-bonding ability at 8 weeks after implantation, although a slight increase was evident beyond 16 weeks. In contrast to these treatments, acid and heat treatments increased bone-bonding ability markedly as early as 4 weeks after implantation, and this increased with time. This marked increase in the bone-bonding ability of Ti metal resulting from acid and heat treatment might have been attributable to apatite formation on its surface in the living body. As shown in Fig. 3, Ti metals subjected to abrasion alone, heat treatment alone or acid treatment alone did not form apatite on its surface in SBF, whereas that subjected to both acid and heat treatment formed apatite on its surface within one day. This indicates that the former three kinds of Ti metals do not form apatite on their surfaces in the living body, whereas the latter one forms apatite even in the living body, as is the case for bioactive ceramics such as Bioglass, glass-ceramic A–W and sintered hydroxyapatite [15]. It is expected that Ti metal, which forms apatite on its surface in the living body, would be able to bond to living bone through the apatite, as is the case for the bioactive ceramics described above [15].

The slight increase in the bone-bonding ability of Ti metal subjected to acid treatment alone at a later stage after implantation might be attributable to some form of transformation of the surface structure to induce apatite formation. On its surface. However, it should be noted that treatment with both acid and heat was much more effective for achieving strong bonding of Ti metal with living bone (see Fig. 4), as well as for forming mature bone on Ti metal (see Fig. 6), than simple acid treatment alone.

Ti metal that has been subjected to acid treatment alone has been used clinically for dental implants, as it shows good osseointegration through its micrometer-scale surface

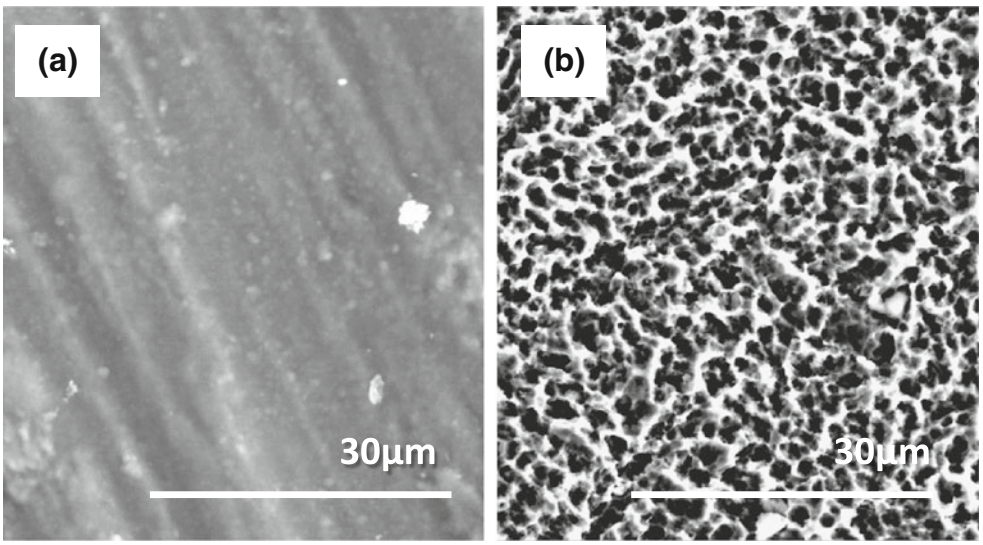

Fig. 9 SEM photographs of the surfaces of 0.5HCl-H and MAH samples retrieved immediately after implantation into the tibia. **a** 0.5HCl-H: the nanometer-scale network has been leveled and has disappeared. **b** MAH: the micrometer-scale surface structure remains unchanged

roughness [24–28]. The present results show that if acid-treated Ti metal is subjected to subsequent heat treatment, it integrates better with the surrounding bone and provides more stable fixation.

The results of the detaching test and histological observations described above suggested that HCl and heat treatments of Ti metal after NaOH treatment also conferred high bone bonding ability, irrespective of the HCl concentration. This high bone-bonding ability might also be attributable to apatite formation on the surface of Ti metals subjected to HCl and heat treatments after NaOH treatment, since these Ti metals form apatite on their surfaces in SBF, as shown in Fig. 3.

However, if bone-bonding ability is determined by apatite-forming ability, then Ti metal subjected to treatment with 50 mM HCl after NaOH treatment would be expected to have bone-bonding ability as high as that of Ti metal subjected to the mixed acid and heat treatments, and higher than that of Ti metal subjected to treatment with 0.5 mM HCl after NaOH treatment, since the former showed apatite-forming ability as high as that of Ti metal subjected to the mixed acid and heat treatments, and higher than that of Ti metal subjected to treatment with 0.5 mM HCl after NaOH treatment (see Fig. 3). In fact, the failure load of the former Ti metal was lower than that of Ti metal subjected to the mixed acid and heat treatment and almost equal to that of Ti metal subjected to treatment with 0.5 mM HCl (see Fig. 4). This could be interpreted in terms of the difference in surface structure between Ti metal simply treated with acid and heat and that subjected to treatment with acid and heat after NaOH treatment.

As can be seen in Fig. 2, Ti metal simply subjected to acid and heat treatment had a dense and rough top surface structure, whereas Ti metals subjected to acid and heat treatments after NaOH treatment had a less dense structure about 1 micrometer thick consisting of feather-like phases near the surface, irrespective of the HCl concentration employed. As a result, the surface structure of the latter Ti metal might tend to be partly destroyed during implantation into a hole created in bone, thus decreasing its apatite-forming ability, whereas the surface structure of the former Ti metal is retained even after implantation. Figures 7, 8, and 9 clearly show that the surface structure of the Ti metals subjected to acid and heat treatments after NaOH treatment was, in fact, partly destroyed after implantation, whereas that of the Ti metal simply subjected to acid and heat treatment was not.

It can be seen from Fig. 3 that Ti metal subjected to acid and heat treatments acquires high apatite-forming ability irrespective of whether it has been previously subjected to NaOH treatment. This high apatite-forming ability cannot be attributed to a specific crystalline phase on the surface of the Ti metal, since the rutile phase of titanium oxide detected on the surface of the Ti metal can also be detected after simple heat treatment, which does not lead to apatite formation. Specific surface roughness is also not responsible for apatite formation, since the surface structure differs considerably between Ti metal subjected simply to acid and heat treatment and that subjected to treatment with acid and heat after NaOH treatment, as described above.

All of the Ti metal subjected to acid and heat treatments exhibited high positive surface charges, as shown in Table 1. Therefore, their high apatite-forming abilities might be attributed to their high positive surface charges. The reasons why Ti metal subjected to acid and heat treatment acquires a highly positive charge in the living

body, and the process of apatite formation on such positively charged Ti metal, have already been discussed elsewhere [16, 17, 29].

5 Summary

The bone-bonding properties of Ti metal subjected to various surface treatments were examined by mechanical detaching test and histological observation after implantation into rabbit tibiae for various periods ranging from 4 to 26 weeks. The following findings were obtained.

1. The bone-bonding ability of Ti metal, which is extremely low as it is abraded, is hardly increased by simple heat treatment at 600 °C or by mixed-acid treatment, at least at an early stage after implantation, whereas it is markedly increased by the heat treatment after the acid treatment, even at an early stage after implantation.
2. Even Ti metal that has been previously subjected to NaOH treatment shows considerably high bone-bonding ability after subsequent acid and heat treatments.
3. The high bone-bonding ability of Ti metal subjected to the acid and heat treatments can be attributed to its high apatite-forming ability in the body environment.
4. The high apatite-forming ability of Ti metal that has been subjected to the acid and heat treatments is attributable to high positive surface charges, and not to the type of crystalline phase or specific roughness of the surface.

These results show that acid treatment and subsequent heat treatment is an effective approach for increasing the bone-bonding ability of Ti metal, thus conferring stable fixation on Ti metal implants.

References

1. Head WC, Bauk DJ, Emerson RH Jr. Titanium as the material of choice for cementless femoral components in total hip arthroplasty. Clin Orthop Relat Res. 1995;311:85–90.
2. Lester DK. Microscopic studies of human press fit titanium hip prostheses. Clin Orthop Relat Res. 1997;341:143–50.
3. Yee AJ, Kreder HK, Bookman I, Davey JR. A randomized trial of hydroxyapatite coated prostheses in total hip arthroplasty. Clin Orthop Relat Res. 1999;366:120–32.
4. McNally SA, Shepperd JA, Mann CV, Walczak JP. The results at nine to twelve years of the use of a hydroxyapatite-coated femoral stem. J Bone Joint Surg Br. 2000;82:378–82.
5. Geesink RG, Hoefnagels NH. Six-year results of hydroxyapatite-coated total hip replacement. J Bone Joint Surg Br. 1995;77:534–47.
6. Moroni A, Toksvig-Larsen S, Maltarello MC, Orienti L, Stea S, Giannini S. A comparison of hydroxyapatite-coated, titanium-coated, and uncoated tapered external-fixation pins. An in vivo study in sheep. J Bone Joint Surg Am. 1998;80:547–54.
7. Bloebaum RD, Beeks D, Dorr LD, Savory CG, DuPont JA, Hofmann AA. Complications with hydroxyapatite particulate separation in total hip arthroplasty. Clin Orthop Relat Res. 1994;298:19–26.
8. Morscher EW, Hefti A, Aebi U. Severe osteolysis after third-body wear due to hydroxyapatite particles from acetabular cup coating. J Bone Joint Surg Br. 1998;80:267–72.
9. Kokubo T, Miyaji F, Kim H-M, Nakamura T. Spontaneous formation of bonelike apatite layer on chemically treated titanium metals. J Am Ceram Soc. 1996;79:1127–9.
10. Kim HM, Miyaji F, Kokubo T, Nakamura T. Preparation of bioactive Ti and its alloys via simple chemical surface treatment. J Biomed Mater Res. 1996;32:409–17.
11. Yan WQ, Nakamura T, Kobayashi M, Kim HM, Miyaji F, Kokubo T. Bonding of chemically treated titanium implants to bone. J Biomed Mater Res. 1997;37:267–75.
12. Nishiguchi S, Fujibayashi S, Kim HM, Kokubo T, Nakamura T. Biology of alkali- and heat-treated titanium implants. J Biomed Mater Res A. 2003;67:26–35.
13. Kawanabe K, Ise K, Goto K, Akiyama H, Nakamura T, Kaneuji A, et al. A new cementless total hip arthroplasty with bioactive titanium porous-coating by alkaline and heat treatment: average 4.8-year results. J Biomed Mater Res B Appl Biomater. 2009;90:476–81.
14. Kokubo T, Kushitani H, Sakka S, Kitsugi T, Yamamuro T. Solutions able to reproduce in vivo surface-structure changes in bioactive glass-ceramic A-W. J Biomed Mater Res. 1990;24:721–34.
15. Kokubo T, Takadama H. How useful is SBF in predicting in vivo bone bioactivity? Biomaterials. 2006;27:2907–15.
16. Kokubo T, Pattanayak DK, Yamaguchi S, Takadama H, Matsushita T, Kawai T, et al. Positively charged bioactive Ti metal prepared by simple chemical and heat treatments. J R Soc Interface. 2010;7(Suppl 5):S503–13.
17. Pattanayak DK, Yamaguchi S, Matsushita T, Kokubo T. Nanostructured positively charged bioactive TiO2 layer formed on Ti metal by NaOH, acid and heat treatments. J Mater Sci Mater Med. 2011;22:1803–12.
18. Pattanayak DK, Kawai T, Matsushita T, Takadama H, Nakamura T, Kokubo T. Effect of HCl concentrations on apatite-forming ability of NaOH-HCl- and heat-treated titanium metal. J Mater Sci Mater Med. 2009;20:2401–11.
19. Nakamura T, Yamamuro T, Higashi S, Kokubo T, Itoo S. A new glass-ceramic for bone replacement: evaluation of its bonding to bone tissue. J Biomed Mater Res. 1985;19:685–98.
20. Takemoto M, Fujibayashi S, Neo M, Suzuki J, Kokubo T, Nakamura T. Bone-bonding ability of a hydroxyapatite coated zirconia-alumina nanocomposite with a microporous surface. J Biomed Mater Res A. 2006;78:693–701.
21. Onishi E, Fujibayashi S, Takemoto M, Neo M, Maruyama T, Kokubo T, et al. Enhancement of bone-bonding ability of bioactive titanium by prostaglandin E2 receptor selective agonist. Biomaterials. 2008;29:877–83.
22. Fukuda A, Takemoto M, Saito T, Fujibayashi S, Neo M, Yamaguchi S, et al. Bone bonding bioactivity of Ti metal and Ti-Zr-Nb-Ta alloys with Ca ions incorporated on their surfaces by simple chemical and heat treatments. Acta Biomater. 2011;7:1379–86.
23. Fujibayashi S, Nakamura T, Nishiguchi S, Tamura J, Uchida M, Kim HM, et al. Bioactive titanium: effect of sodium removal on the bone-bonding ability of bioactive titanium prepared by alkali and heat treatment. J Biomed Mater Res. 2001;56:562–70.
24. Klokkevold PR, Nishimura RD, Adachi M, Caputo A. Osseointegration enhanced by chemical etching of the titanium surface. A torque removal study in the rabbit. Clin Oral Implants Res. 1997;8:442–7.
25. Pebe P, Barbot R, Trinidad J, Pesquera A, Lucente J, Nishimura R, et al. Countertorque testing and histomorphometric analysis of

various implant surfaces in canines: a pilot study. Implant Dent. 1997;6:259–65.
26. Sullivan DY, Sherwood RL, Mai TN. Preliminary results of a multicenter study evaluating a chemically enhanced surface for machined commercially pure titanium implants. J Prosthet Dent. 1997;78:379–86.
27. Baker D, London RM, O'Neal R. Rate of pull-out strength gain of dual-etched titanium implants: a comparative study in rabbits. Int J Oral Maxillofac Implants. 1999;14:722–8.
28. De Leonardis D, Garg AK, Pecora GE. Osseointegration of rough acid-etched titanium implants: 5-year follow-up of 100 minimatic implants. Int J Oral Maxillofac Implants. 1999;14:384–91.
29. Pattanayak DK, Yamaguchi S, Matsushita T, Kokubo T. Effect of heat treatments on apatite-forming ability of NaOH- and HCl-treated titanium metal. J Mater Sci Mater Med. 2011;22:273–8.